Implementing Digital Feedback Controls

for the Multiple Simultaneous Ring Cavities

in the FASOR-X System

Jeffrey T. Baker, David Gallant, Arthur Lucero

Boeing-LTS, Albuquerque, NM

Harold Miller, Jonathon Stohs

AFRL, KAFB, NM

AMOS CONFERENCE 2011

Abstract

Precision tuned high power (~50W) 589nm generation for use in laser sodium guidestar generation is a key capability in today's modern adaptive optical systems. The approached used is Sum-Frequency Generation (SFG) of 1319nm and 1064nm lines of Nd:YAG in an LBO crystal. High power narrow line sources are not commercially available, so low power narrow-band NPRO sources are mated with resonantly tuned high power ring lasers to achieve high power pumps. Efficient conversion of 589nm requires high pump intensities within the LBO crystal, therefore a doubly-resonant ring cavity is used. Four implementations of the Pound-Drever-Hall method are applied to achieve these. Finally, precision wavelength tuning is required to generate the correct wavelength as measured by a Wavemeter and verified by a low pressure Na-cell. These multiple control loops are all interconnected, to some degree, with various physical requirements, constraints, and caveats. Like any worthwhile project, the systems integration of the control systems has been an educational endeavor.

1.   INTRODUCTION

Sodium laser guidestar D2a-exciting sources are in world-wide demand as an essential ingredient to state-of-the-art Adaptive Optical (AO) optical systems whose purposes are to mitigate the effects of the atmosphere by using an artificially-created "guidestar" as a reference [1,2].

We discuss here in particular the multiple coupled servo controls of the FASOR-X system (Frequency Addition via the Sum of Optical Radiation, rev. X, also commonly referred to as the "Generation 1.5 FASOR") as built by our team. This system is a highly re-engineered, refined, and repackaged version of the original FASOR device[2,3,4]. As can be seen in figure 1 below, the FASOR-X system is part of a larger AO system, and consists of subsystems in 3 physical locations, with various interconnects, including the FASOR-X box which is mounted directly on the telescope and rotates with the azimuthal bearing. This system from the beginning was engineered specifically for the AMOS 3.67m telescope's unique requirements.
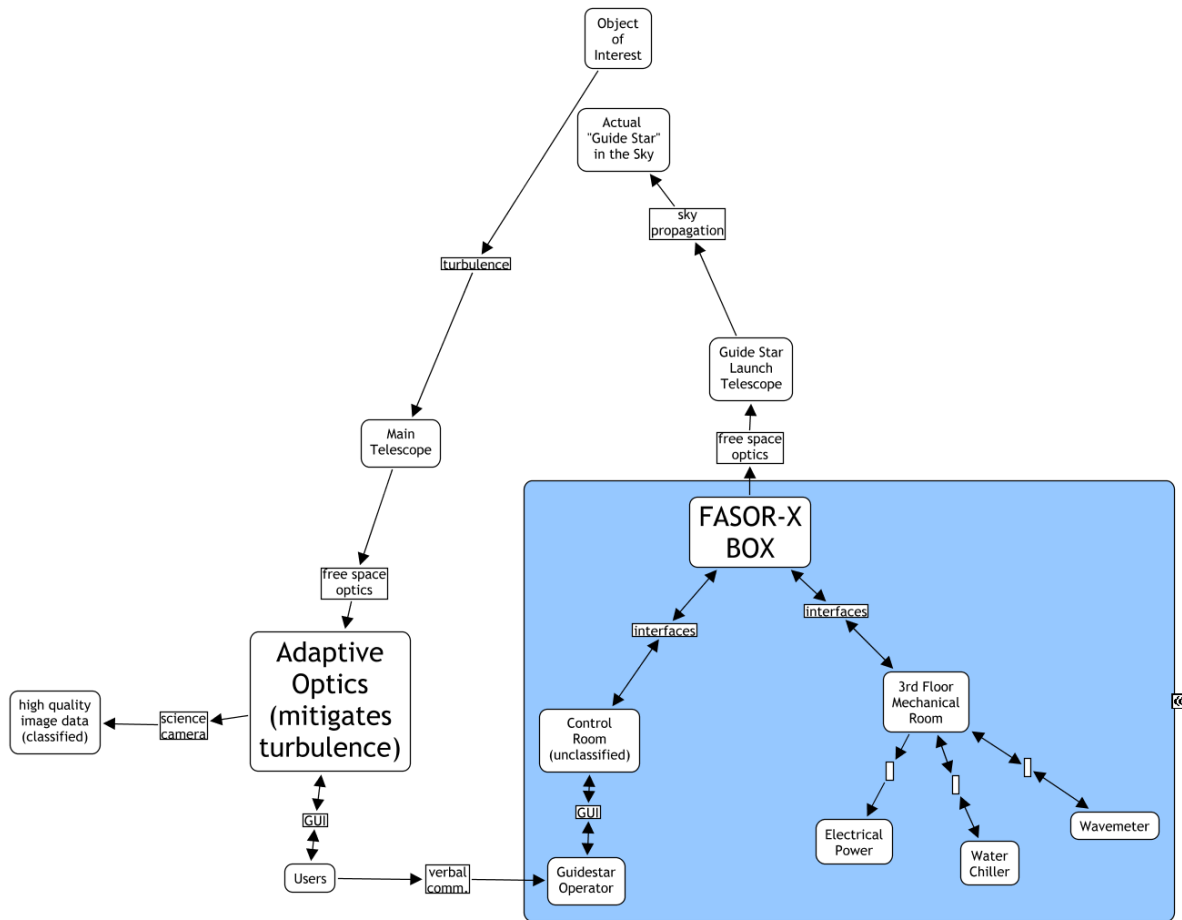

Figure 1 FASOR-X SYSTEM LOCATION CONCEPT MAP

As we peer into the FASOR-X box itself in figure 2, we see that this is a version of the highly complex yet proven FASOR technology first developed and used at the Starfire Optical Range. This notional diagram shows the larger

subsystems within the box, which includes a pair of embedded controllers, a pair of high power, narrow-band, injection-locked ring oscillators, and a doubly-resonant optical sum-frequency generator cavity.
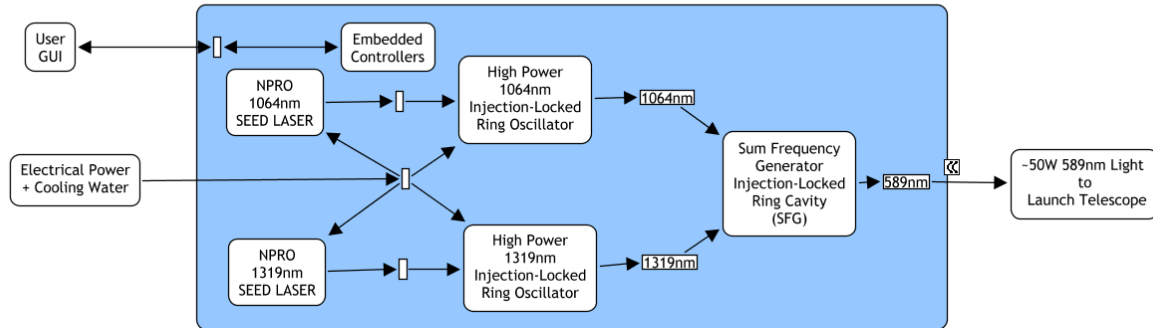

Figure 2 FASOR-X BOX BLOCK DIAGRAM

Figure 3 shows how the components are laid out at some level of detail, showing the main components of a) 1064nm and 1319nm NPRO seed lasers, b) 1064nm and 1319nm high powered ring oscillator modules with water flow manifolds integrated, and c) the long rear cold plate where all of the controllers and electronics are locally mounted.
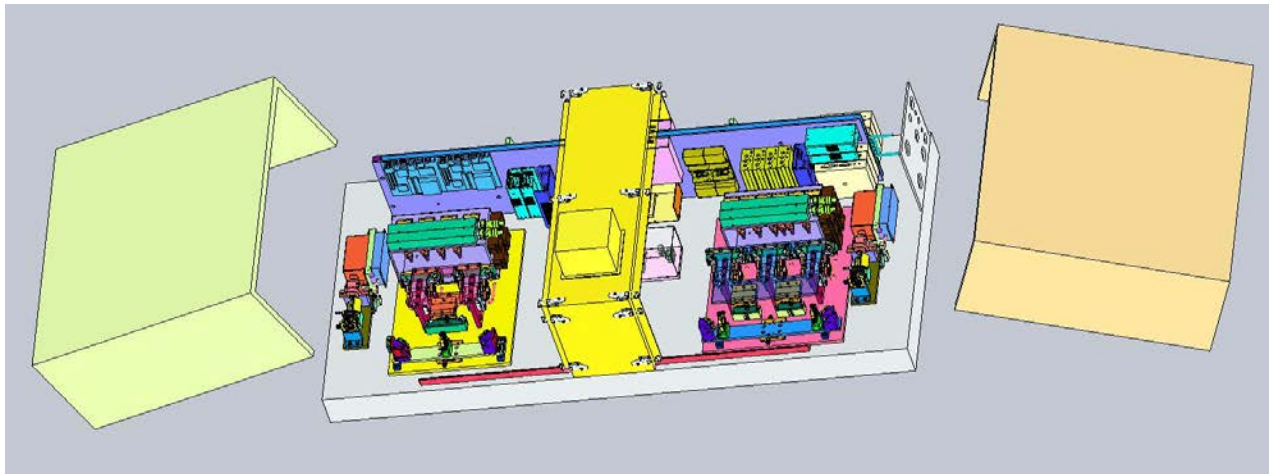

Figure 3 FASOR-X BOX RENDERING

2. CONTROLS

Figure 4 shows the control diagram for the six critical control loops, four of which are based on the high speed Pound-Drever-Hall(PDH) sensing method explicitly developed for ring cavity locking. The remaining two loops are

to control the wavelengths of the two NPRO seed sources so that the exact wavelength of 589nm can be achieved and maintained.
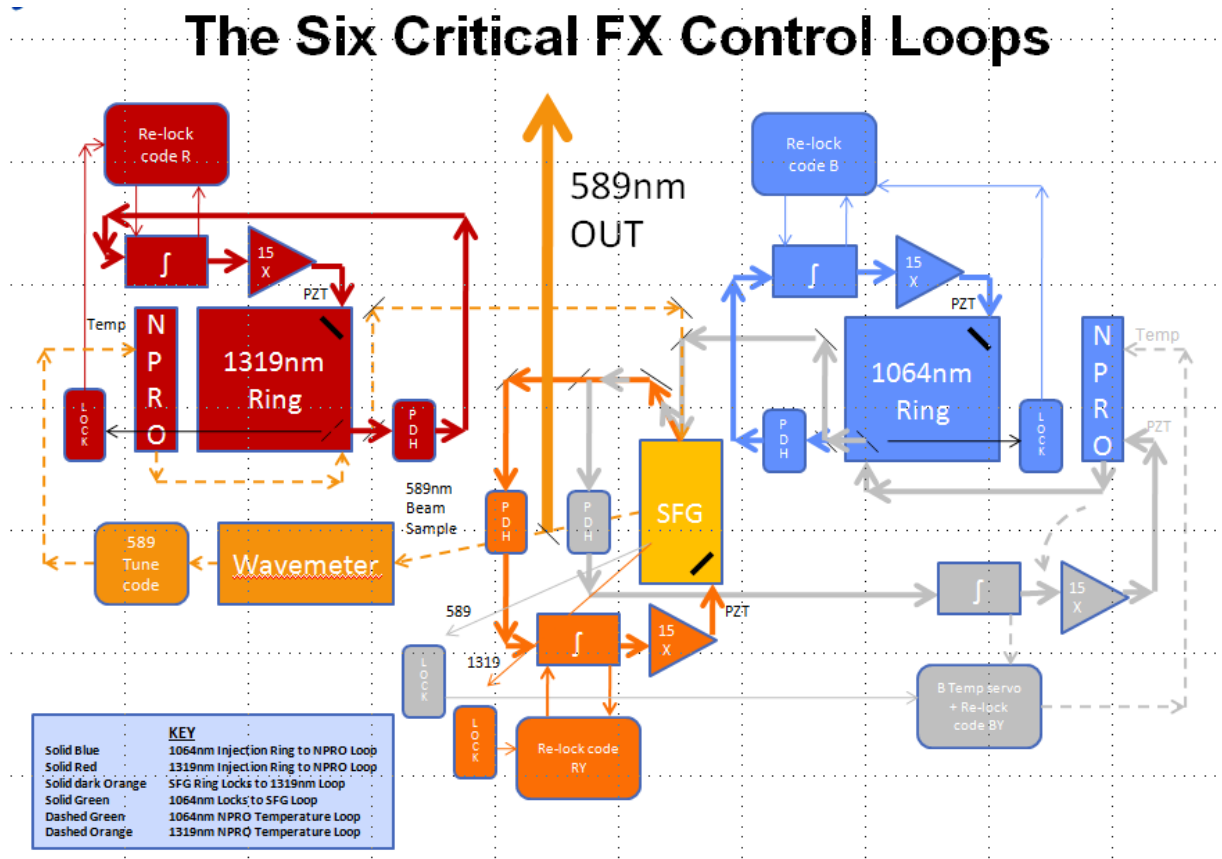

Figure 4 FASOR-X CONTROL SYSTEM DIAGRAM

Figure 5 shows the basic PDH error-sensing method for injection locked ring cavities [6], which in variations is applied 4 times in the FASOR-X system. Careful selection of RF components, EO modulators, analog preamplifiers, filters, and servo control circuitry are required for robust locking due to the complex shape and highly non-linear nature of the PDH error signal.
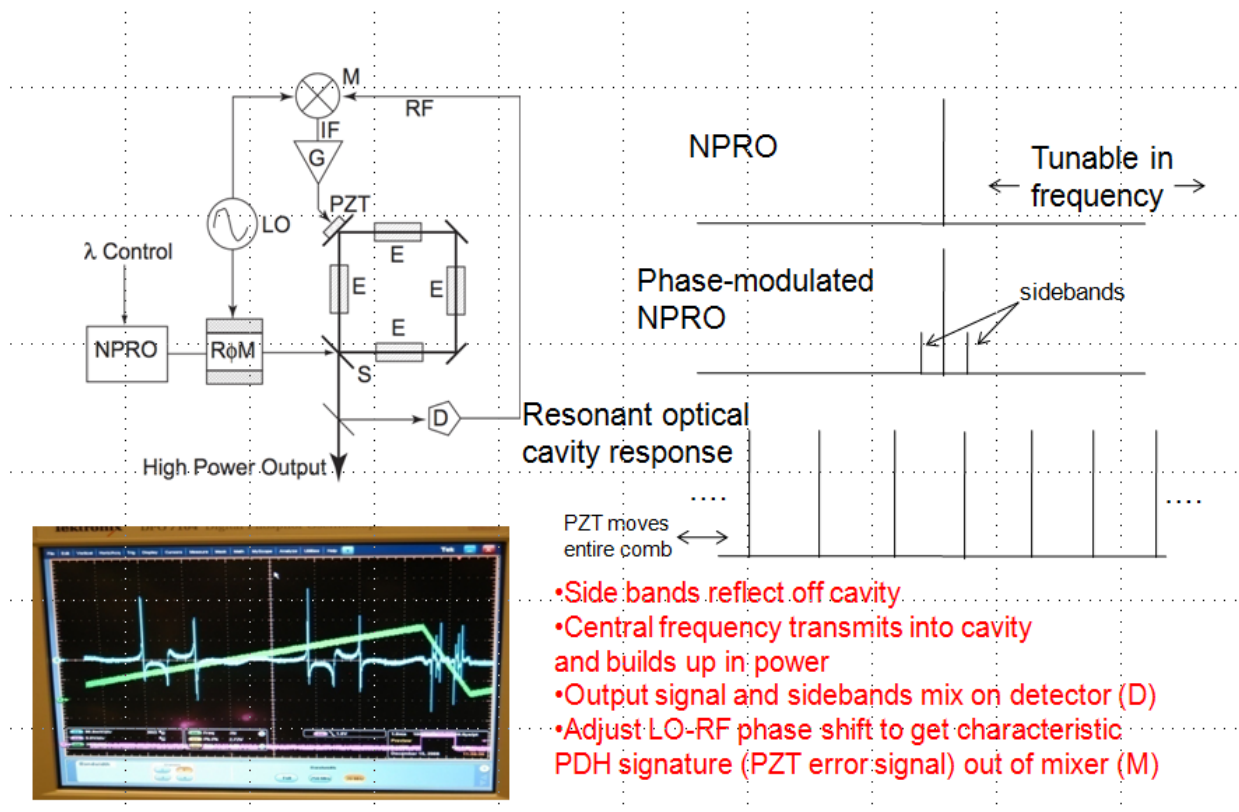
Figure 5 TYPICAL POUND-DREVER-HALL DETECTION SCHEME

While the PDH error signal is in general quite complex, a linearized model can be constructed to validate performance of the feedback control loops for the small but useful parts of this curve (resonant positive sloping zero-crossing region in-between two anti-resonant negatively sloping zero crossings). Figure 6 shows how the system behaves for one of the typical fast loops when the single integral gain servo parameter is varied. The circuit is limited by the 50 kHz damped resonance of the PZT displacement mirror (the plant) within the ring cavity. Attempting to increase the speed by setting K>0.3 results in oscillatory behavior, whilst values of K<0.1 prove to be too sluggish in some cases. In actuality, each of the 4 loops has its own optimum gain region due to a) the nature of the individual disturbances to be compensated in terms of amplitude and frequency content, and b) the resonances of the individual PZT, c) the electro-mechanical coupling between the PZT and other mirror structures (not modeled here), and d) the individual cavity optical finesse, higher finesse being more difficult. Other factors include the PDH excitation frequency, the particular cavity's free spectral range, and this loop's photo-receiver SNR, which varies. Some complex coupling of loops occurs and must be de-coupled by either clever design or adequate bandwidth separation of loops. The loops lock in the order of a) both ring lasers lock to their NPRO seeds, simultaneously, via the rings' piezos, then b) the SFG locks onto the 1319nm high powered source using its piezo, followed by c) the 1064nm high powered ring source locks onto the SFG via the internal 1064nm NPRO piezo and d) temperature setting, and finally, the 1319nm temperature is slowly scanned (with all other loops tracking) until the wavemeter reads the correct 589.15905nm for the D2a line. Some of the loops are coupled as a result of the 589nm conversion, making the choices for gains and detector saturation and trip levels critically important. For example, some absorption within the LBO crystal or its heated holder may cause transient optical path difference shifts, which can cause end-of-travel errors in the SFG loop. Situations such as this must be avoided.

From a controls standpoint the most difficult task of all perhaps is that of setting up the software systems to scan for and locate the optical path differences which will put each of the loops into its proper part of the PDH curves simultaneously, with the ability to ignore unimportant glitches and quickly correct for others. Otherwise, the entire "house-of-cards" falls down and no 589nm light is emitted, or, just as inappropriately, the wavelength will shift off of the D2a line. Also, for each loop there are multiple lock points, and some are definitely better than others. The lock/re-lock software algorithm must take this in to account using all available information to move to the correct lock points no matter which loop is in jeopardy. The result is that while the overall locking and re-locking scheme is complex, each loop, in the end, runs on its own initiative, with care taken so that no loop gets in the other's way.

Originally, an all-digital system was envisioned to handle the 4 critical realtime loops using a 100kS/S sample rate. DAQ format and size issues limited the sample rate at first to 40kS/S, then down to 20kS/S to maintain signal integrity due to crosstalk and the need to interleave dead channels. Then, interactions of the sampled system with the PZT and other electro-mechanical resonances made the solution somewhat less robust than had been hoped. The solution was to add a single analog integrator (with hard range limits) implemented as a single inexpensive quad-operational amplifier to the system to provide >100kHz of analog bandwidth for the servo component, while letting the computer modify their behaviors at a more modest 20kS/S. Robustness increased dramatically while maintaining computer to control of the locking and re-locking process, and actually simplifying the control law. While a 10 kHz control loop rejection bandwidth was the specification, we achieved 35kHz with this simple modification on the loops which needed it the most.
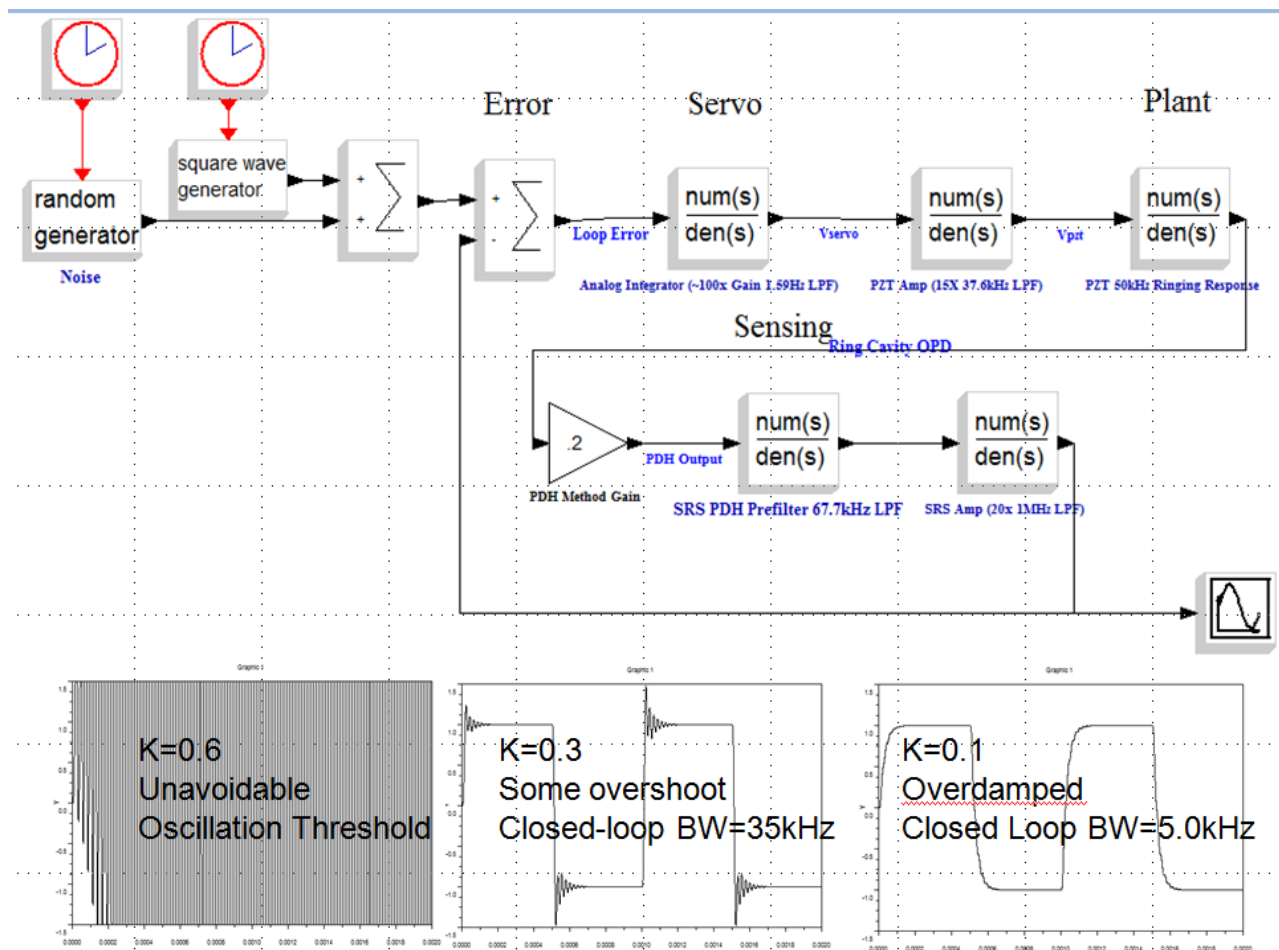

Figure 6 FASOR-X TYPICAL PDH LOOP SIMULATION RESULTS

Figure 7 shows a notional graphical user interface for the FASOR-X device. Normally, the operator will have little to do in order to activate the system: 1) activate the chiller; 2) activate the SFG heater; 3) turn on the Main System Software via a single click and wait 10-20 minutes for the system to produce 589nm power and thermally settle; and 4) verify that the system is at 589.15905nm using the wavemeter and adjust the wavelength if necessary. As a rule, locking is automatic and only takes at most a few seconds, requiring no operator intervention. Re-locking is usually much faster if not nearly instantaneous in the FASOR-X system.
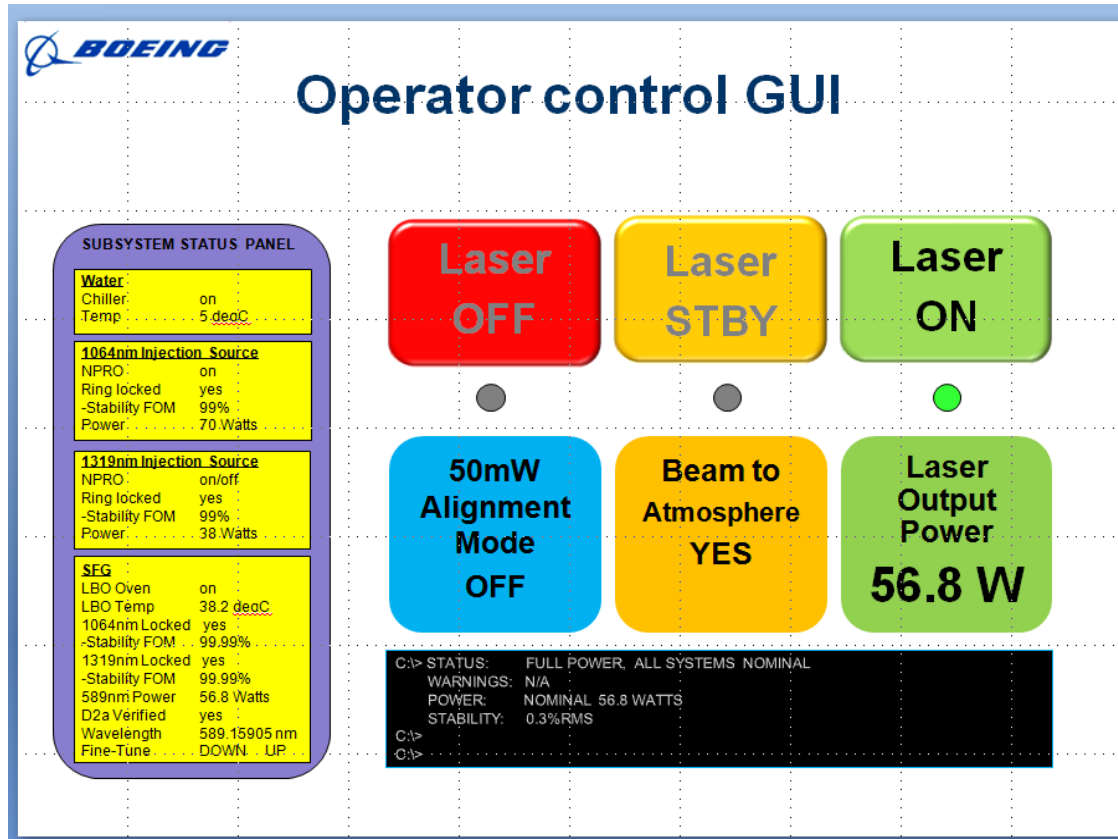

Figure 7   FASOR-X GUI

3. CONCLUSIONS

Figure 8 shows the actual system while running (cover removed) at >55Watts of 589nm output power. Some simple arithmetic shows that the conversion efficiency for the light applied to the SFG cavity (1064nm + 1319nm) with LBO crystal was >75%, while for light entering the SFG cavity it was impressive at >95%. Although the output beam quality is yet to be measured, it appears to be very nearly perfect (see lower right inset, figure 8). The 55W power limitation is due to running out of 1319nm power in this case, as we had over 20W of 1064nm power to spare when these data were taken and maintained over several days.

Achieving these results is a story in and of itself, with multiple subtle optical, mechanical, vibrational and electronics issues having to be resolved along the way. These results show the high quality of the injection ring sources pumping the SFG, and low losses in conversion process due to excellent mode-matching, excellent alignments and excellent locking of all servos. Engineering reliable high power, high beam quality, narrow line

sources is challenging [5]. New technology was invented in order to increase injection ring power and beam quality, etc. in the face of unexpected Cr+ rod doping in the 10ea. diode-pumped laser engines, for example.

And, most of all, we thoroughly enjoyed the technical challenges and wealth of knowledge gained while developing this state-of-the-art FASOR system.
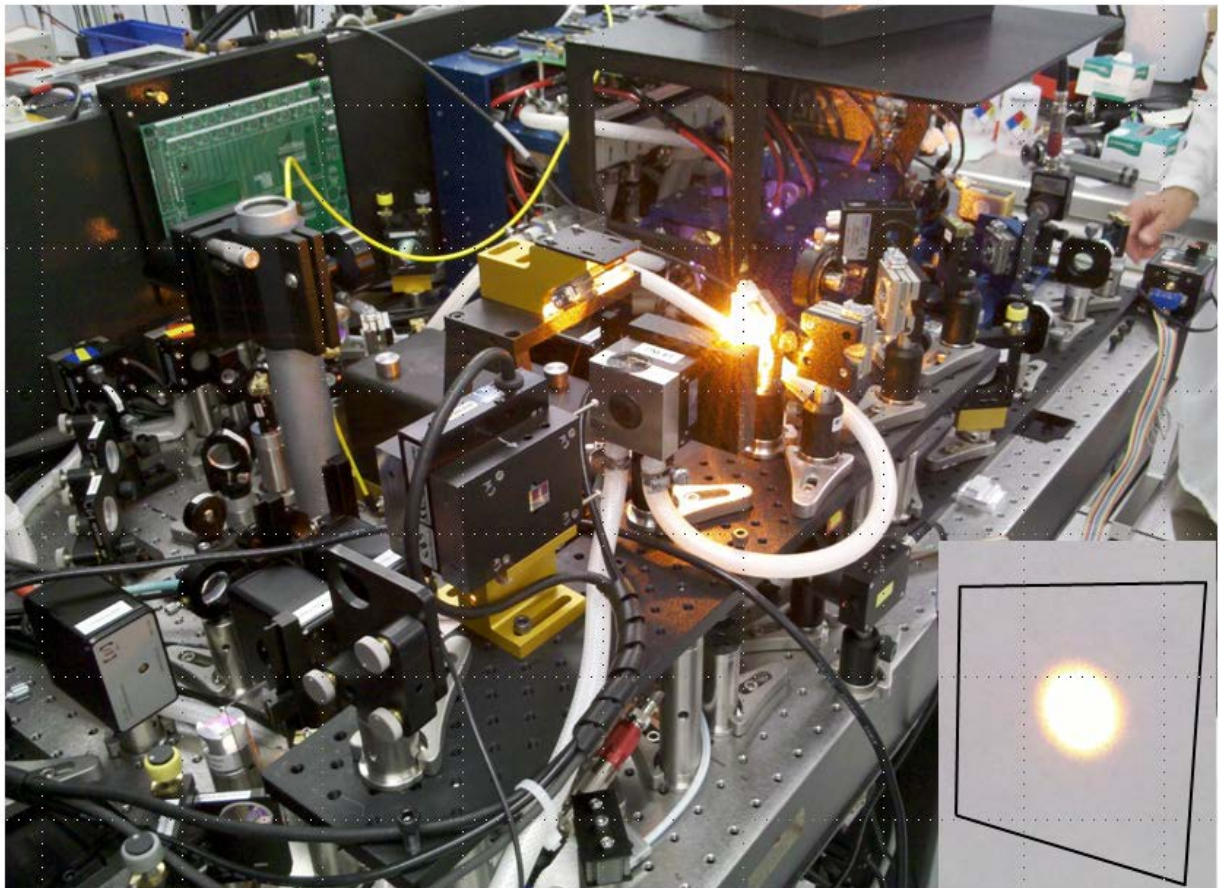

Figure 8 FASOR-X SYSTEM DURING HIGH POWER OPERATION

4. REFERENCES

1. Baker, J., Gallant, D., Lucero, A., Miller, H., Stohs, J., Novel All Digital Ring Cavity Locking Servo, AMOS Conference 2009.
2. Denman, C., Drummond, J., Eickhoff, M., Fugate, R., Hillman, P., Novotny, S., Telle, J. Characteristics of sodium guidestars created by the 50-watt FASOR and first closed-loop AO results at the Starfire Optical Range, Proc. of the SPIE, Vol. 6272, pages 62621L-1 through 62621L-12.
3. Fugate, R., Denman, C., Hillman, P., et. al., Progress toward a 50-Watt facility-class sodium guidestar pump laser, Proceedings of the SPIE Vol. 5490, pages 1010-1020.
4. Denman, C., Hillman, P., Moore, G., Telle, J., et. al., Realization of a 50-Watt facility class sodium guidestar pump laser, Proceedings of the SPIE Vol. 5705, pages 46-49.
5. Advanced LIGO homepage: http://www.ligo.caltech.edu/advLIGO/
6. Black, Eric D., An Introduction to Pound-Drever-Hall laser frequency stabilization, Am. J. Phys. 69 (1), January 2001.